Separation Science and Technology
Publication details, including instructions for authors and subscription information:
http://www.informaworld.com/smpp/title~content=t713708471

Characterization of an Improved Electropolarization Chromatographic System Using Homogenous Proteins

E. N. Lightfoot[a]; P. T. Noble[a]; A. S. Chiang[a]; T. A. Ugulini[a]
[a] CHEMICAL ENGINEERING DEPARTMENT, ENGINEERING BUILDING 1415 JOHNSON DRIVE UNIVERSITY OF WISCONSIN MADISON, WISCONSIN

To cite this Article Lightfoot, E. N. , Noble, P. T. , Chiang, A. S. and Ugulini, T. A.(1981) 'Characterization of an Improved Electropolarization Chromatographic System Using Homogenous Proteins', Separation Science and Technology, 16: 6, 619 — 656
To link to this Article: DOI: 10.1080/01496398108058120
URL: http://dx.doi.org/10.1080/01496398108058120

SEPARATION SCIENCE AND TECHNOLOGY, 16(6), pp. 619-656, 1981

Characterization of an Improved Electropolarization Chromatographic System Using Homogenous Proteins

E. N. LIGHTFOOT, P. T. NOBLE, A. S. CHIANG, and T. A. UGULINI

CHEMICAL ENGINEERING DEPARTMENT
ENGINEERING BUILDING
1415 JOHNSON DRIVE
UNIVERSITY OF WISCONSIN
MADISON, WISCONSIN 53706

ABSTRACT

A critical examination of Electropolarization Chromatography, EPC, shows the first-order model currently used to be inadequate. Marked deviations from expectation are observed, especially at low buffer concentrations, and these may result in either higher or lower retardation than expected. Specific interactions between the protein and buffer, separate from effects of pH and ionic strength, are evident, as well as specific interaction between the protein and fiber wall. More refined data acquisition and analysis yields measurements of dispersion which tend to be larger than predicted.

A multicomponent transport model is developed which qualitatively predicts much of these observed effects. This modeling effort gives added insight for design and optimization of EPC columns.

INTRODUCTION

The Nature of Electropolarization Chromatography (EPC) and Its Relation to Other Separation Processes

We use the term EPC here to denote a specialized form of electrical field-flow fractionation using a hollow cylindrical

fiber rather than parallel sheets to confine the solutes to be separated. It is thus a specialized type of chromatographic separation taking place within a single fluid phase and dependent to an unusual degree on non-uniform fluid motion. It will be described in some detail below, but general familiarity with the chromatographic and field flow fractionation literature will be assumed. Those wishing a more detailed introduction are referred to the recent review of Lightfoot, Chiang, and Noble (7).

A. Nature

In polarization chromatography retardation is produced primarily by concentration polarization within a non-uniform flow field. In electropolarization chromatography, described in Figure 1, polarization is accomplished by electrophoretic migration against a semipermeable membrane, and the non-uniform flow is a slightly distorted Poiseuille velocity distribution.

In this process a buffered electrolyte flows continuously down the lumen of a permselective hollow fiber, and separation is initiated by injecting a pulse of protein solution into this stream over a short time interval. The protein is quickly concentrated into a lens-shaped region adjacent to the inner fiber wall by a balance between electrophoretic migration and concentration diffusion. This is indicated by the shading in the top view of Fig. 1. The protein is also moved axially, by convection at the local fluid velocity. Since the velocity near the wall is low, mean axial velocity of the protein pulse, $\langle v_{pz} \rangle$, is less than that of the carrier (buffer) solution: the protein is retarded by the polarization process. Separation of two proteins occurs if they are polarized to different degrees. Clearly this is an inherently transient, hence chromatographic, process, and we have found that it can be described successfully by the equation

$$\frac{\partial \bar{c}_i}{\partial t} + \langle v_{iz} \rangle \frac{\partial \bar{c}_i}{\partial z} - \varepsilon_{im} \frac{\partial^2 \bar{c}_i}{\partial z^2} + \bar{c}_i \frac{\partial \langle v_{iz} \rangle}{\partial z} = 0 \qquad (1)$$

Here c_i is local molar concentration of species i, and v_i is the observable velocity of i resulting from directed fields or forces and bulk fluid motion; ε_{im} is the effective dispersion coefficient of i through the mixture of species present, and z is the direction of flow; t is time. The overline and brackets represent averaging defined by

$$\bar{c}_i = \frac{1}{s}\int_s c_i ds \tag{2}$$

$$\langle v_i \rangle = \int_\tau c_i v_i d\tau / \int_\tau c_i d\tau \tag{3}$$

Here s is system flow cross-section and τ is volume.

In general, however, both $\langle v_{pz} \rangle$ and ε_{pm} must be considered functions of time - as well as the physico-chemical nature of the system. Much of the work outlined below is aimed at relating these quantities to buffer composition, flow conditions, geometry, and other factors to be discussed.

B. Historical aspects and relation to other polarization processes

The concept of combining intraphase concentration polarization with non-uniform convection is an old one, and it does not seem feasible to seek its true origin. Many variants, using gravitational and centrifugal fields, have long existed in the mineral industry (13), and attempts at polarization separation of proteins go back at least to Kirkwood (4).

Most closely related to EPC are a group of polarization processes collectively known as field-flow fractionation, developed and extensively investigated by J.C. Giddings and his associates (see Lightfoot et al. 1981 for a recent review of these techniques). These differ geometrically from EPC in an apparently trivial but actually quite important way in using flow between parallel planes rather than in cylindrical ducts. In addition some polarization processes, for example thermal and centrifugal field flow fraction-

ation, do not require mass to pass across the polarizing surfaces. This will be seen to have a profound effect on system behavior.

Our research group was led rather naturally to the development of polarization induced separations by an attempt to put the troublesome polarization of proteins in ultra-filtration apparatus to use. As a result we were the first, by a small margin, to report ultrafiltration induced polarization separations, similar to the flow field flow fractionation of Giddings et al.

It is, however, quickly apparent that two separation mechanisms are particularly selective and flexible for fractionation of biologically active proteins: thermodynamic activity gradients (usually in the form of selective precipitation or adsorptions) and electrostatic potential gradients (electrophoretic migration).

Our interest centered on preparative aspects of electrophoresis because of the strength of electrophoretic forces and the sensitivity of electrophoretic mobility to buffer concentration, pH, and chemical nature, as well as to poorly investigated properties such as dielectric constant. However, it soon became clear that preparative-scale electrophoresis, for example free-flow electrophoresis, suffered from some inherent defects, e.g. ohmic heating, hydrodynamic instability, and Taylor diffusion (convective dispersion).

Hollow-fiber electropolarization processes offer a number of advantages for electrophoretically based separations of proteins: the use of a small cylindrical geometry

1) eliminates hydrodynamic instability essentially completely, because of the small Rayleigh numbers encountered.
2) permits high degrees of concentration polarization, hence strong retardation, without appreciable ohmic heating, because of small dimensions and the very high ratio of Schmidt to Prandtl numbers in aqueous protein solutions.
3) greatly reduces Taylor diffusion, because the thickness of diffusional boundary layers adjacent to the polarizing barrier is typically quite small. (though in

practice non-idealities limit the degree to which one can realize this potential).

4) provides automatic control of shape.

These advantages appear to justify a major developmental effort, and experience has tended to bear out this expectation. However, as discussed in the next section, the apparent simplicity of this process is in many ways deceptive, and experimental results often deviate quite markedly from expectations based on the simple models so far available. Some of these deviations are disadvantageous, and means must be sought to minimize them; others are potentially useful and should be increased. In the next section we summarize what is presently known about this process.

THEORY

Quantitative Description of EPC and Assessment of Its Potential Utility

In this section we review mathematical and experimental descriptions of EPC developed to date and discuss the significance of these developments, both to our understanding of this process and to its potential as a separations tool. Among the most important characteristics of any chromatographic process are solute retardation and dispersion, and, because these have been most thoroughly studied to date, they will dominate our discussion. Other important characteristics include column productivity and the range of solutes which can be effectively separated in a single column. These will be discussed to a limited extent here, but they are still largely subjects for further research.

A. The mathematical basis of description and first-order models

Rather complete differential descriptions both for fractionations of true molecules (particles, such as small colloids, may be treated as molecules provided Basset forces and other inertial

effects are unimportant), based on the generalized Stefan-Maxwell equations (6), and for hydrodynamic particles are available (7). For true molecules subjected only to chemical and electrical forces, and with negligible diffusional interactions, this description reduces, for any species i in solvent s, to:

$$\frac{\partial c_i}{\partial t} - (\nabla \cdot \underset{\sim}{N}_i) = 0 \tag{4}$$

$$\text{with } \underset{\sim}{N}_i = cx_i\underset{\sim}{v}_i \triangleq cx_i(\underset{\sim}{v}_s + \underset{\sim}{v}_F) = cD_{is}\nabla x_i \tag{5}$$

$$\underset{\sim}{v}_F \triangleq - D_{is}(\nabla \ell n\gamma_i + \frac{m_i}{D_{is}} \nabla\phi) \tag{6}$$

Here in addition to terms previously defined $\underset{\sim}{N}_i$ is the molar flux of species i in fiber fixed coordinates, D_{is} is the effective pseudobinary diffusivity of i relative to the solvent, γ_i is the thermodynamic activity coefficient of i, m_i is electrophoretic mobility, and ϕ is electrostatic potential; ∇ is the gradient operator.

Equation 4, the continuity equation, is exact in the absence of chemical reactions (which can occur for native protein but which we shall ignore in this discussion). Equation 5 may be considered a definition of the migration velocity $\underset{\sim}{v}_F$, in which case all approximations are made in Eq. 6 (7).

The most important boundary condition is that on the inner wall of the fiber N_{pr}, the radial component of the protein flux, is zero. Proper specification of boundary conditions and equations of state are major problems still to be solved.

Even this simplified description is formidable, and, with one exception (12), all published analyses neglect polarization of all species but the protein in question - and also the variation of γ_i and D_{is} with position and time. They also assume Poiseuille flow, thus failing to account for the effect of protein polarization on local viscosity.

The most reliable and complete of such simplified descriptions are those of Lee et al. (5) for slit flow, Takashi and Gill (14)

for rectangular channels of finite aspect ratio, and Reis et al. (9) for Poiseuille flow (circular flow cross-sections). All are obtained from generalizations of the Taylor-Gill-Subramanian dispersion theory as provided by Lee et al. (15), and, for Poiseuille flow, via the generalized Sturm-Liouville theory of Ramkrishna and Amundson (8). All of these results can be summarized most completely by a modification of Eq. 1 in which migration velocity and dispersion coefficients are time dependents

$$\frac{\partial \bar{c}_p}{\partial t} + \frac{\bar{v}_m}{r_p}\frac{\partial \bar{c}_p}{\partial z} = \varepsilon_p \frac{\partial^2 \bar{c}_p}{\partial z^2} \tag{7}$$

where

$$\bar{c}_p = \frac{1}{s}\int_s c_p ds = \text{area-mean value},$$

$r_p = r_p(t)$ = retardation coefficient for species p, $= \bar{v}_m/\bar{v}_p$

$\varepsilon_p = \varepsilon_p(t)$ = effective axial diffusivity for species p,

$\bar{v}_m$ = average velocity of total fluid.

Complete description of transient behavior is provided in the above references.

The transient contributions to r_p and ε_p can be important, but very considerable insight can be gained from examining long-time limiting behavior:

$$(r_p)_\infty \equiv \lim_{t\to\infty}\{r_p\} \tag{8a}$$

$$(\varepsilon_p)_\infty \equiv \lim_{t\to\infty}\{\varepsilon_p\} \tag{8b}$$

These quantities in turn are functions only of geometry and the polarization Péclet number

$$Pe = \frac{v_F B}{D_{is}} \tag{9}$$

and B is the radius of lumen or the half-width of a planar channel; v_F is the migration velocity of Eq. 6. For high degrees of polari-

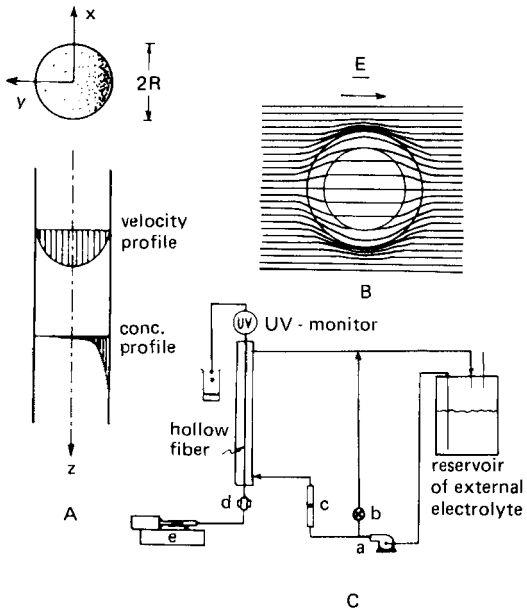

FIGURE 1. Hollow-fiber EPC: (A) coordinate system, convection-velocity profile, and equilibrium-concentration profile in the hollow fiber, with the dotted region representing the lens-shaped concentrated protein region; (B) distortion of the electrical force lines due to the presence of an isotropic cylindrical duct; (C) sketch of the experimental setup: (a) external buffer pump; (b) bypass valve; (c) flow meter; (d) hollow fiber; (e) syringe pump.

zation, or large $P\acute{e}$, $(r_p)_\infty$ and $(\varepsilon_p)_\infty$ can be approximated by simple asymptotic expressions. Asymptotic retardations are given by

$$(r_p)_\infty = P\acute{e}/3 \qquad \text{(slits, large } P\acute{e} \text{ limit)} \qquad (10)$$

$$= P\acute{e}/4 \qquad \text{(tubes, large } P\acute{e} \text{ limit)} \qquad (11)$$

where the corresponding dispersion coefficient for both geometries is approximately

$$(\varepsilon_p)_\infty = \frac{8(v_0 B)^2}{D_{ps} P\acute{e}^4} \left(1 - \frac{5}{P\acute{e}} + \frac{7}{P\acute{e}^2}\right), \qquad (12)$$

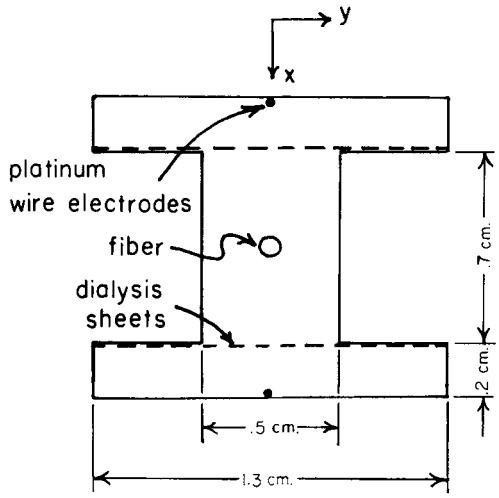

FIGURE 2. Cross-section of the EPC fiber chamber.

where v_o is the maximum axial fluid velocity. These results must be applied cautiously in slit flow, because numerical calculations by Takahashi and Gill (14) indicate surprisingly large side effects for finite horizontal-aspect ratios. If borne out experimentally this prediction illustrates one more major effect of geometry.

Other expressions for retardation and dispersion are also widely used. For example the solute retardation is expressed by Giddings in terms of retention ratio, R:

$$R = \frac{1}{r_p} \quad . \tag{13}$$

In the chromatography literature, the height of an equivalent theoretical plate, H, is commonly used to express dispersion. In terms of Giddings' notation, H is calculated by the following equation

$$H = 4B^2\lambda^2\psi\ \bar{v}R/D + \frac{2D}{\bar{v}} \tag{14}$$

where

$$\lambda = \frac{1}{2P\acute{e}} \tag{15}$$

$$\psi \triangleq 4(1-6\lambda) \text{ for small } \lambda. \tag{16}$$

The plate height can be related to ε_p by

$$\frac{HR}{B} = \frac{2\varepsilon_p}{\bar{v}B} \tag{17}$$

where the right-hand side is equivalent to a reciprocal, effective, axial Péclet number.

RESULTS AND DISCUSSION

Experimental Observations

A rather extensive experimental survey of EPC has already been made, with particular emphasis on the parameters of primary importance to chromatographers: solute retardation and dispersion. We have also made some preliminary tests of field programming, which is unusually simple and flexible for this process, and we have begun to investigate the effects of concentration and other parameters on protein transport properties. Finally we have begun to assess the potential of EPC for separations of practical interest. These activities are reviewed briefly here.

A. Apparatus and Procedures

The experimental system used in our studies is shown schematically in Fig. 1. The heart of this system is the test cell containing the hollow fiber and electrodes. A 50-cm long fiber is mounted on stainless steel needles and oriented linearly inside the test cell. Two platinum wire electrodes are aligned parallel to the fiber as shown in Fig. 2. Dialysis sheets serve to insulate the fiber compartment from the electrolysis products. Important auxilliary equipment for the buffer circulating as shown

in Fig. 1 include a Harvard model 901 syringe pump and a 10 μl Altex sample injection valve connected to the fiber with teflon microbore tubing. A teflon-gear micro pump circulates buffer from the electrodes to the reservoir. For operation at currents up to 1 ampere, the reservoir is immersed in a controlled temperature water bath, and connected to a vacuum source of $6 - 9 \times 10^4$ Pa. in order to remove electrolysis products. The proper volumetric flow rates and pressures of the circulating system are maintained by the throttling valves shown in Figure 1.

The ultra filtration fibers are experimental prototypes obtained from Amicon Corporation, Lexington, Mass. and three different types have been used: P5, YC and YM. The YM fibers have the highest electrical conductivity, and the smallest tendency to adsorb proteins. Most of the data reported here utilize this type. The YM type has an inner radius of approximately 0.03 cm.

Ovalbumin was obtained from Sigma Chemical Co. as grade V. Human serum albumin (HSA) was obtained from Miles Laboratory pentex label. Hemoglobin was prepared in our laboratory from clinical blood samples using the chromatographic method of Schnek and Schroeder (11) with No. 6 developer. Types A_{II} and A_{IC} human hemoglobin were isolated and behaved identically in our apparatus. All buffers were prepared from analytical grade reagents, and characterized by their pH and electrical conductivity.

Protein samples were prepared following dissolution, by dialysis overnight in the appropriate buffer, and by centrifugation to remove undissolved solids. Their concentrations were determined spectrophotometrically using the following extinction coefficients: ovalbumin, $\varepsilon_{280} = 0.75$ cm²/mg; HSA, $\varepsilon_{280} = 0.66$ cm²/mg; and hemoglobin, $\varepsilon_{415} = 8.0$ cm²/mg. Ovalbumin and hemoglobin were examined and found to be electrophoretically pure, whereas HSA was contaminated with oligomers. Monomer HSA was isolated by gel exclusion chromatography and stabilized with iodoacetamide which blocks sulfhydryl groups. This preparation behaved identical to pentex HSA in EPC.

The elution of proteins is currently detected by a dual beam absorbance monitor, model UA5 with type 6 optical unit, from Instrumentation Specialties Company (ISCO). Absorbances of HSA and ovalbumin are detected at 280-310 nm, whereas hemoglobin is detected at 405 nm. The unit also is equipped with a small flow cell (4 μl total volume) which reduces the amount of mixing of the chromatographic peaks, such that most of the dispersion is usually in the ultrafiltration fiber.

Data acquisition, storage, and analysis of elution peaks has been taken over by a mini-computer, the North Star Horizon. Absorbance readings from the ISCO are taken every twenty seconds and stored for further processing. Computer analysis of an elution peak yields the first four moments and the mass balance.

Axial luminal flow measurements can now be monitored continuously by employing a Statham UC3 universal transducer equipped with the UL5 microscale accessory which continuously weighs the aqueous solution eluting from the fiber. The density of the eluate is assumed to be constant at 1 g/cm^3. This signal is sampled by the Horizon computer every twenty seconds, and the change in mass is averaged over 5 minute intervals to compute the flow rate. For the YM fibers, it was found necessary to measure the pressure outside the fiber with a water manometer and the pressure in the fiber line with pressure transducers in order to monitor pressure differences for prevention of ultrafiltration. External buffer circulation was measured with a flowmeter installed as shown in Fig. 1.

The electric field outside the fiber (E_o) is calculated from the observed current density,

$$E_o = J/K \tag{18}$$

where J is the average current density at the center plane of EPC cell and K is the solvent conductivity. Electric fields within the fiber have been estimated using the solution of Laplace's equation for an isotropic hollow cylinder in a uniform field. The ratio of electrical fields inside and out is

$$E_i/E_o = \frac{4}{2 + K/Km + Km/K + \frac{R^2}{(R+\delta)^2}\left(2 - \left(\frac{K}{Km} + \frac{Km}{K}\right)\right)} \qquad (19)$$

where δ is the wall thickness, and Km is the fiber conductivity. Our measurements of Km for YM fibers, (employing an annular conductivity cell), indicates that E_i/E_o is essentially one and assumed to be one in our data analysis.

B. Retardation

The retarding effect of electric fields on protein elution is the easiest parameter to study, and in our early experiments it was the only one measured. Our earliest results, typical examples of which are shown in Fig. 3, were made with P5 fibers. As suggested by the figure, these data tended to conform to model prediction at low fields, but retardation always increased faster than predicted with increasing field, and became essentially infinite at a critical field strength specific to each protein and buffer. The effect is reversible in that the protein is released, except for some ubiquitous irreversible adsorption, on relaxation of the field. This phenomenon, which we refer to as electro-retention, is clearly beneficial, but we have as yet no satisfying explanation for it.

More recently we have been using a new series of fibers, Amicon YC and YM, which exhibit much lower irreversible protein adsorption but which tend to give marked negative deviations from our first-order theory. This is illustrated in Fig. 4 for human serum albumin in 4mM tris acetate buffer at pH 8.3 in YC fibers. It appears from the marked differences between observations with YC and P5 fiber types that electro-retention may not be an entirely appropriate term: this is not entirely an electrical phenomenon.

The complexity of electro-retention is further indicated in Fig. 5 for human serum albumin at different protein loadings and ionic strength. Careful examination of the two uppermost curves in this figure will show that the total amount of electro-retained protein is almost independent of the amount fed to the fiber. We

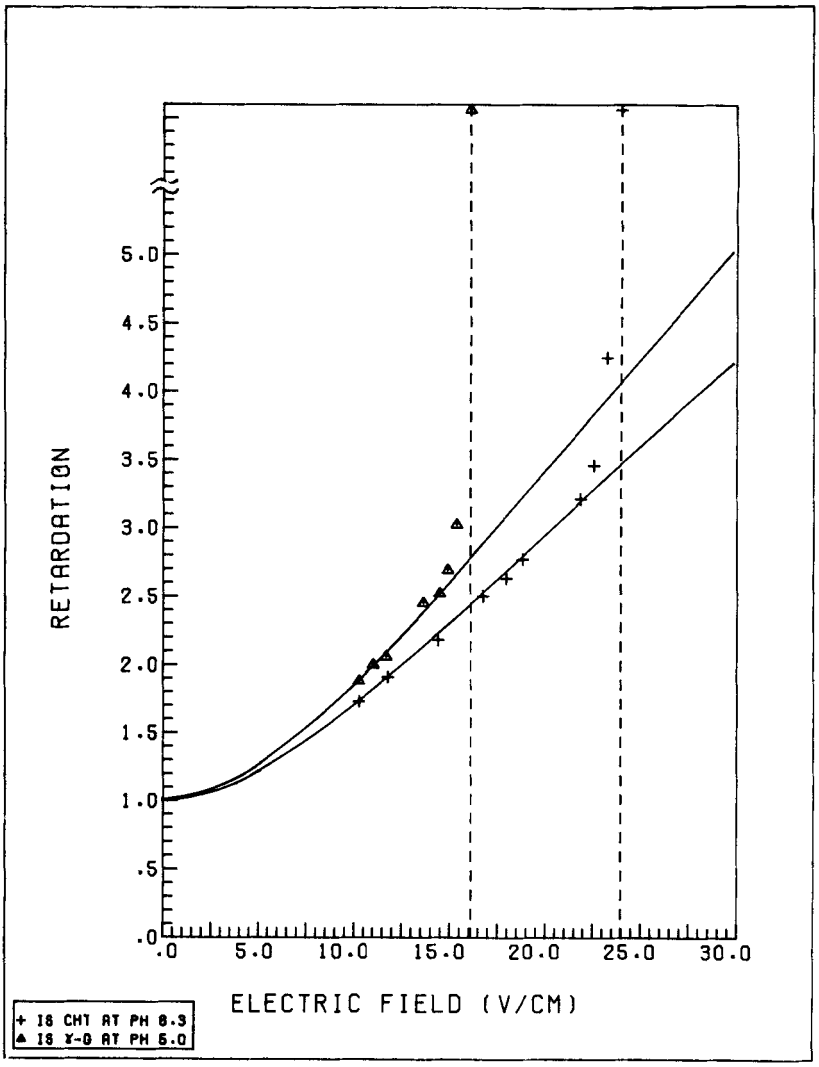

FIGURE 3. Retardation coefficients vs. electrical field for chymotrypsinogen A (CHT) at pH 8.3 in tris 0.001M and bovine gamma globulin (γ-G) at pH 5.0 in sodium succinate 0.001M. The values for the electrical field were calculated from applied voltages, V, by means of equation $E = \alpha V$ with $\alpha = 0.29\ cm^{-1}$, obtained from calibration with human serum albumin and γ-G in barbital 0.001M at pH 8.6. The values for m_i/D_{im} used to plot the theoretical curves were $30\ v^{-1}$ for gamma globulin and $25\ v^{-1}$ for chymotrypsinogen A. The figure shows that after some critical electrical field there is a sharp departure of experimental data from the prediction. The two data points on top of the plot correspond to peaks which were recovered only after the voltage was turned to zero. Data points were obtained with polysulfone fibers. (Reis and Lightfoot (9)).

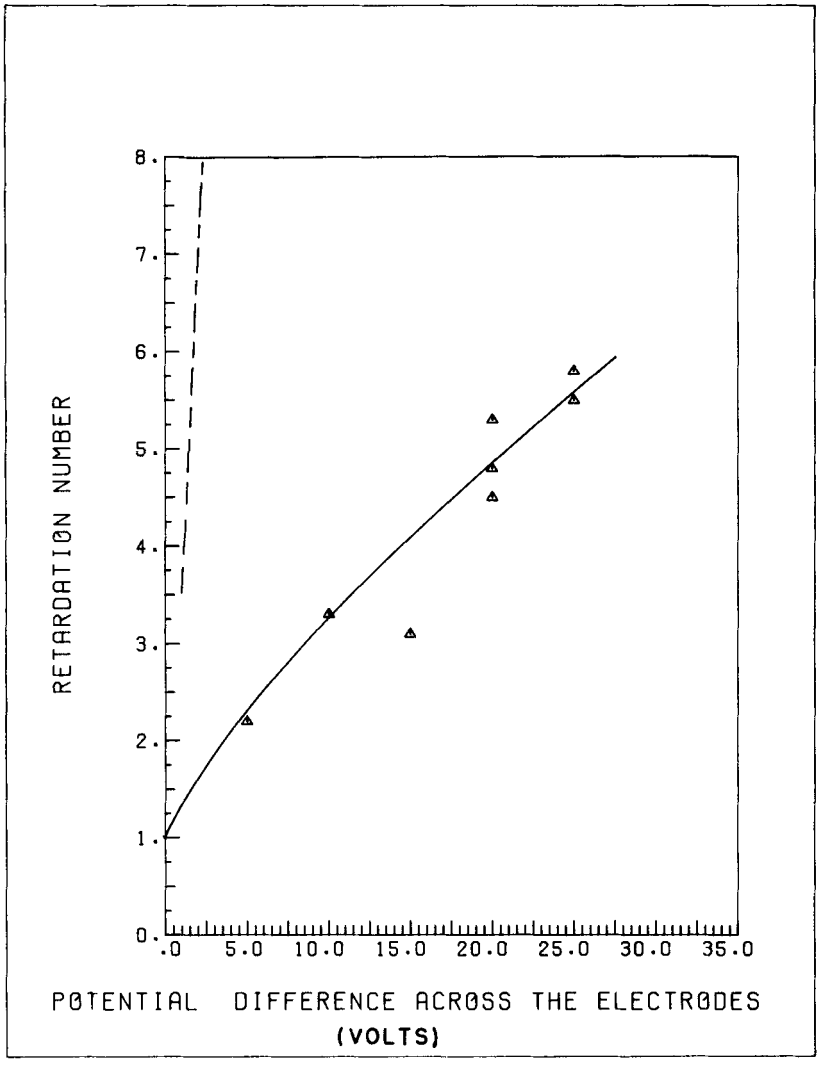

FIGURE 4. Retardation coefficients vs. applied potential difference for human serum albumin in 4mM tris-acetate buffer at pH 8.3, using YC fibers. The dashed line is a theoretical prediction using equation 11 with m_p/D_{pm} for HSA equal to 456 v^{-1}. The electric field is approximated as the potential difference divided by the electrode spacing, 1.1 cm. (Chiang, et al. (1)).

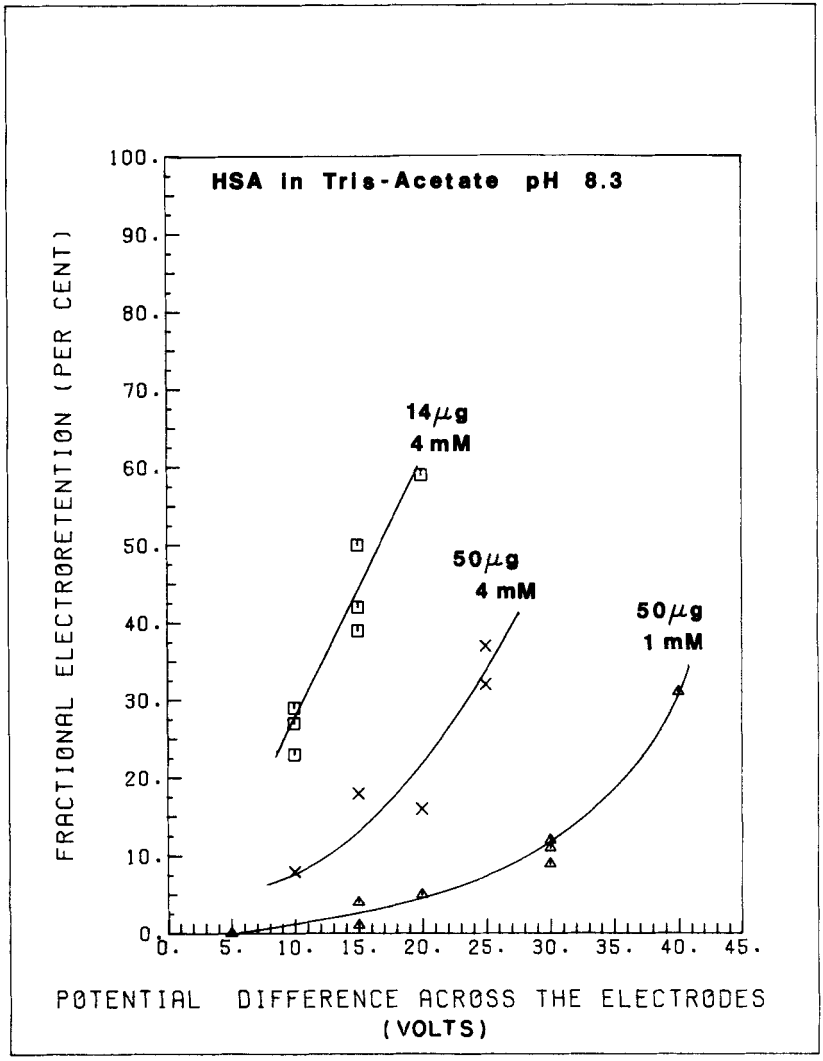

FIGURE 5. Fractional electroretention as a function of the potential difference across the electrodes. Data points were obtained with cellulosic fibers (YC Type). (Chiang, et al. (1)).

have also found that human serum albumin can be quite effectively electro-retained very close to its iso-electric point.

As shown in Fig. 6, for ovalbumin in YM fibers buffer ionic strength has a major effect on retardation, and the observed behavior is qualitatively opposite to that predicted from the first-order theory: Increasing buffer concentration is found experimentally to produce greater retardation rather than less. The incremental change becomes less at higher concentrations, however, and most of the potential benefit appears to be achieved at 20 mM for this system. Possible reasons for this behavior are discussed below, in connection with development of a second-order theory. Similar behavior is observed for hemoglobin in tris acetate, as shown in Fig. 7.

Internal electric fields for YM fibers were calculated from the external field and the measured electrical resistance of the fiber wall. We have every reason to consider such calculations quite reliable.

These two figures suggest that we can approach agreement with first-order theory simply by increasing buffer concentration. Such increases of ionic strength cause greater ohmic heating, however, and can suppress differences in mobility between proteins. Our second-order modelling efforts suggest that the negative deviation from first-order theory results primarily from polarization of buffer constituents. This small-ion polarization can be caused both by the protein boundary layer and a fixed charge in the fiber. In our discussion below we suggest that we may be able to improve retardation at low ionic strengths by modifying fiber properties. We have found the electric properties of the fibers to be sensitive to conditions of manufacture, probably because pore size and density, and ionic character, change.

The mass of protein fed to the fiber also has an effect on retardation not predicted by first-order theory, but the nature of the effect depends in a complex manner on the buffer used. In those buffers yielding the most favorable retardations, an increase in protein loading decreases retardation. This is shown in Fig. 8, for ovalbumin in 10 mM sodium acetate, and Fig. 9, for human serum

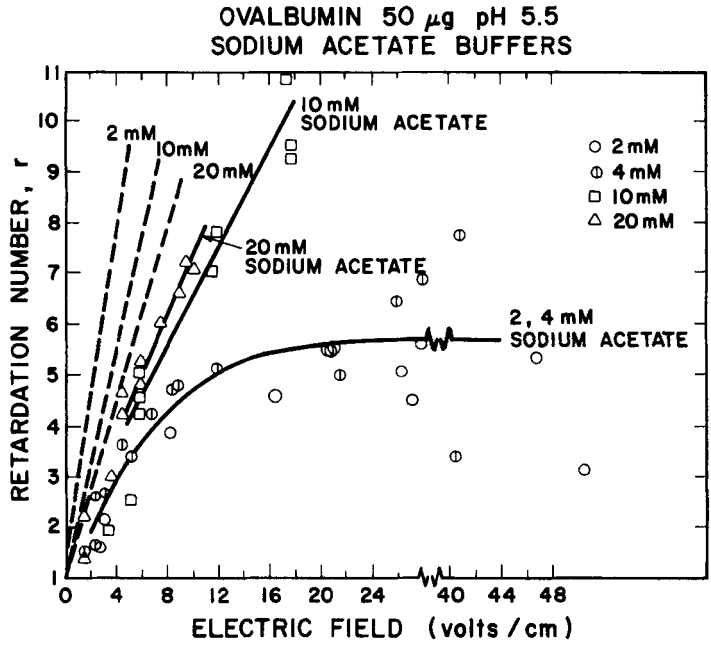

FIGURE 6. Retardation of ovalbumin as a function of electric field. The dashed lines are theoretical predictions, using equation 11, and the mobility and diffusivity of the protein are for the limiting case of infinite dilution. The three lines correspond to three values of the ionic strength used in correcting mobilities to the proper buffer strength, with Henry's Equation. Data points were obtained with cellulosic fibers (YM type).

albumin in tris acetate. However, in some poor buffer-protein combinations the reverse is true. Such a situation is shown in Fig. 10, for hemoglobin in morpholine acetate at pH 8.3. We are not yet in a position to predict the success of protein-buffer systems. In some situations we have been unable to detect any loading effect; these include ovalbumin at 25-500 μg loading in 2-4 mM sodium acetate at pH 5.5 and hemoglobin at 2-50 μg in 20 mM tris acetate at pH 8.3.

C. Dispersion

Control of dispersion is extremely important for obtaining efficient separations, and here EPC has some inherent advantages:

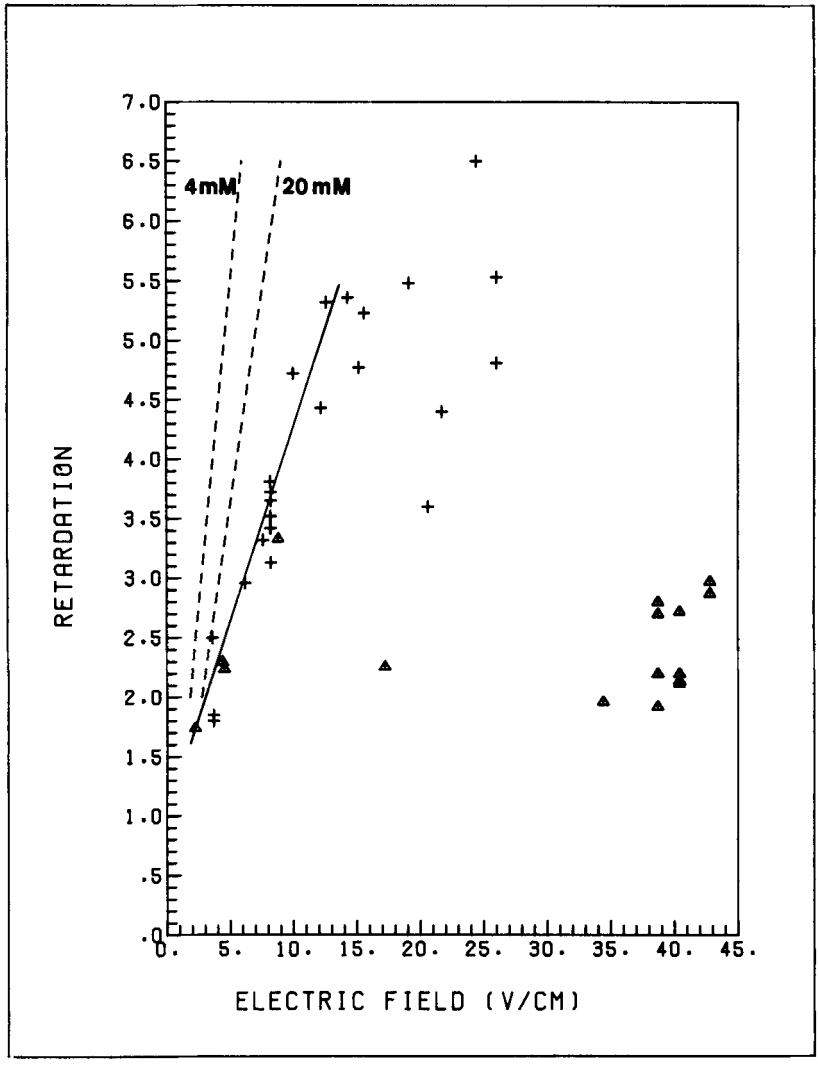

FIGURE 7. Retardation of hemoglobin as a function of electric field in tris acetate buffers at pH 8.3. The dashed lines are predictions by equation 11, at the two buffer concentrations used, 4 and 20 mM. Fair agreement with prediction is observed below 15 v/cm. + is in 20 mM. tris, Δ is in 4 mM tris. (YM fibers).

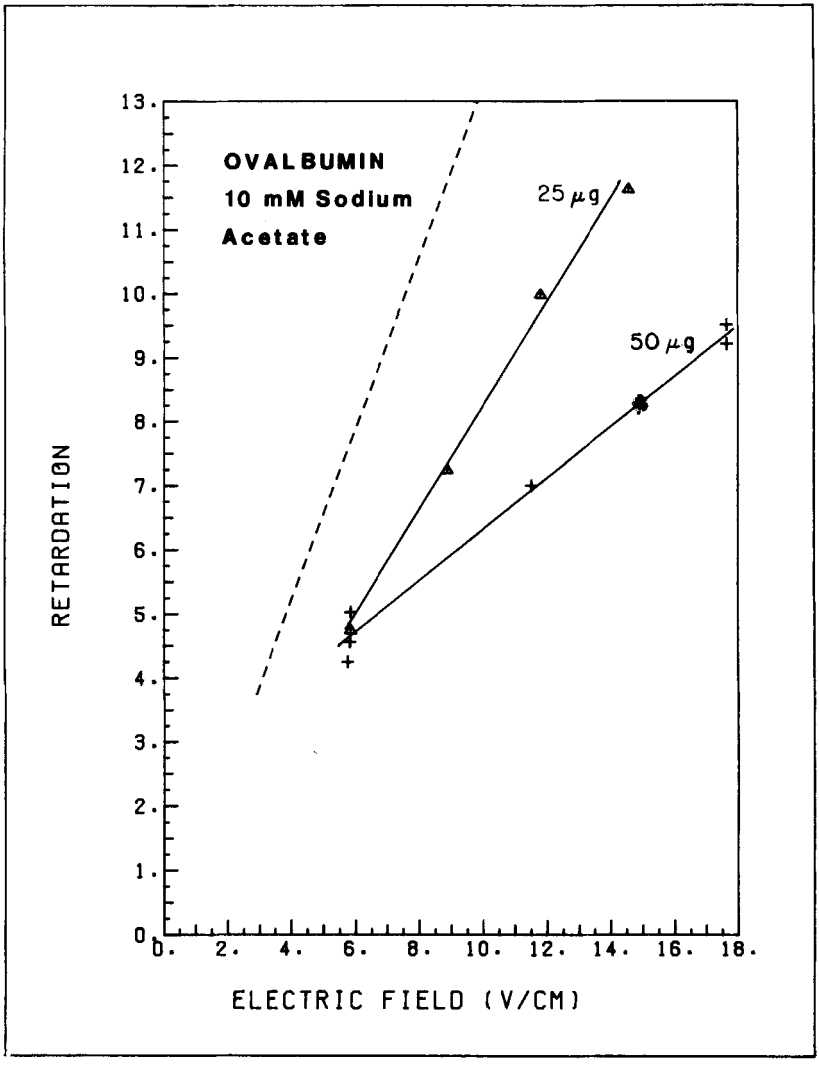

FIGURE 8. The effect of electric field on retardation for two protein loadings. The points are for ovalbumin in 10 mM sodium acetate at pH 5.5 for protein changes of 25 and 50 μg to a YM fiber. The dotted line is the prediction of first order theory using a diffusivity of 7.76×10^{-7} cm^2/sec and mobility of 9.85×10^{-5} cm^2/sec-v.

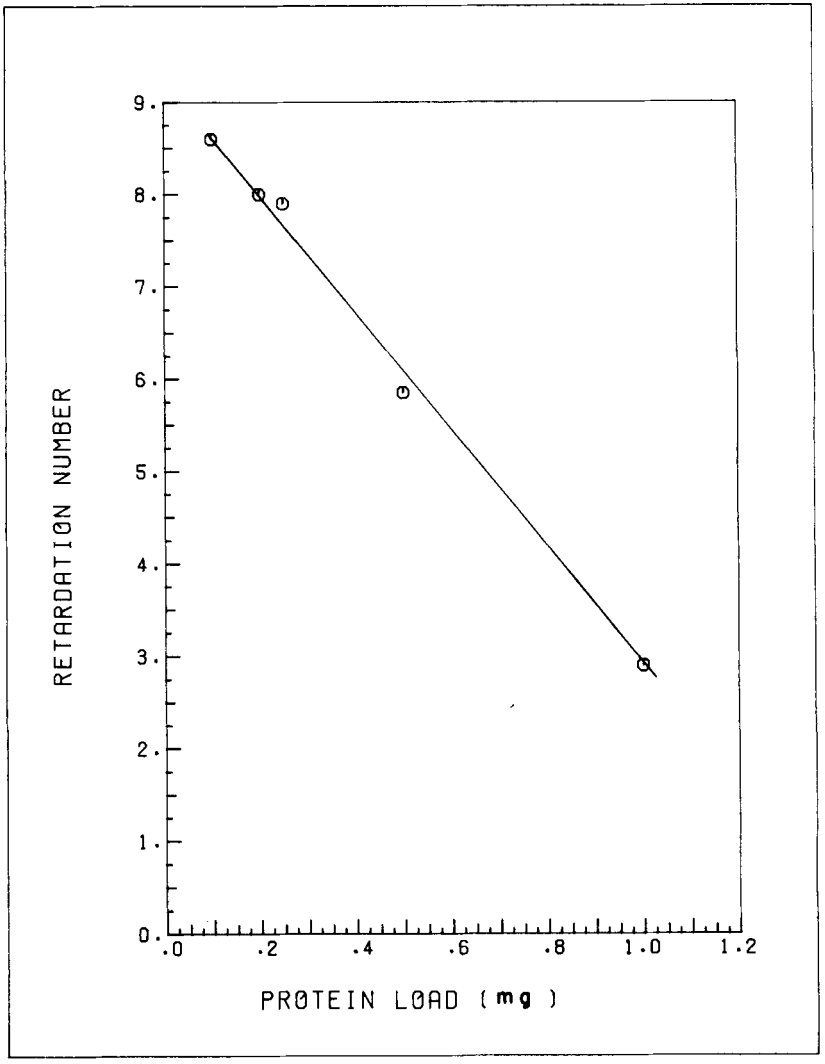

FIGURE 9. The effect of protein loading on retardation. These data were obtained for human serum albumin for 4 mM tris acetate at pH 8.3 in a 280 cm. YM fiber (Chiang et al. (1)).

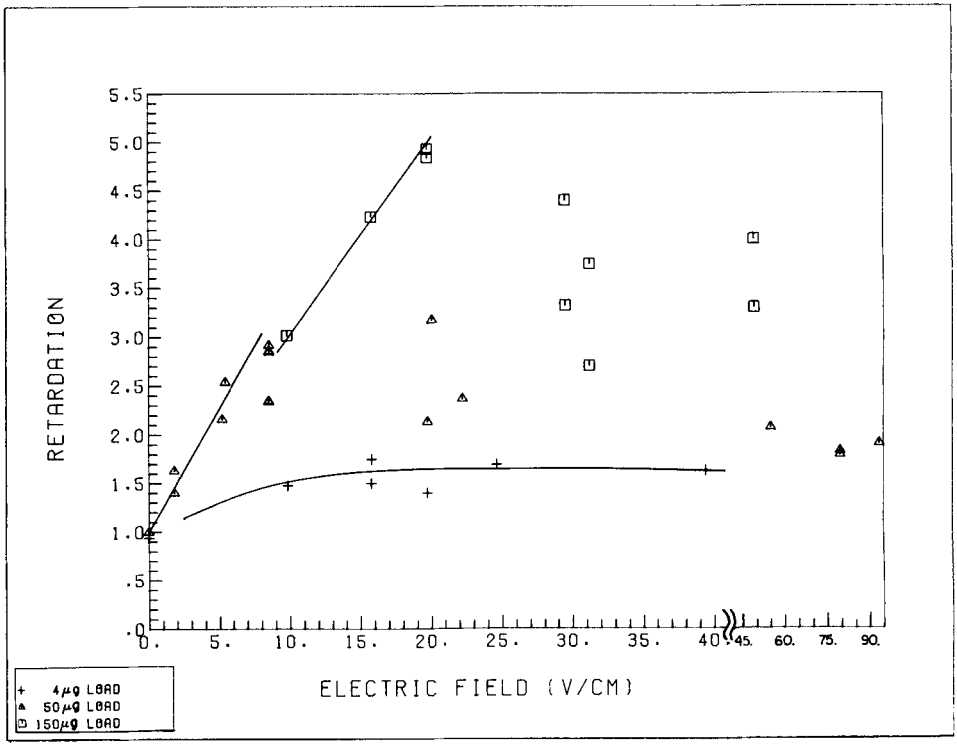

FIGURE 10. The effect of electric field on retardation of hemoglobin in 10 mM morpholine acetate buffer at pH 8.3, for several protein loads.

There is no interphase transfer resistance, since we have only one active phase, and convective dispersion is greatly reduced, at least in principle, by concentrating the protein into extremely thin boundary layers. This is suggested in Fig. 11 which shows scaled axial dispersion coefficients as a function of polarization Péclet number, as calculated from our first-order theory. For no polarization, Pé = 0, axial dispersion is just predicted by the classic dispersion theory of G.I. Taylor: Taylor diffusion. Dispersion then increases moderately with Pé, because of the increasingly non-uniform concentration profile, until solute begins to concentrate into a thin boundary layer near the wall. There is

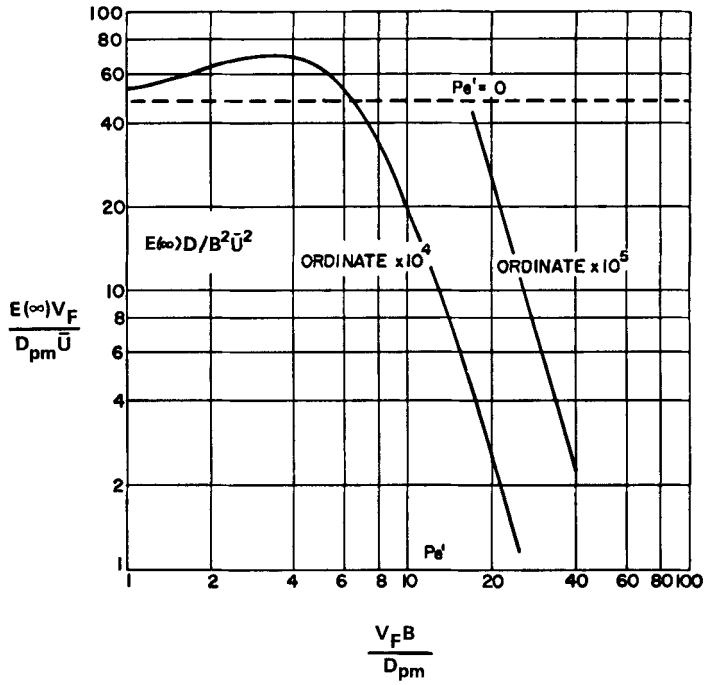

FIGURE 11. Asymptotic axial dispersion as a function of Péclet number. (Lee et al. (5)). Here

$\varepsilon(\infty)$ = asymptotic (maximum) value of axial dispersion coefficient

$\mathcal{D}_{pm}$ = effective binary diffusivity of protein

B = inner fiber radius, for a circular cross-section, or half-width for a slit

$\bar{u}$ = mean axial velocity of buffer in fiber lumen

v_F = migration, here electrophoretic, velocity caused by the polarizing field, see Eq. 6.

then a strong decrease of $(\varepsilon_p)_\infty$ with further increase in Pé, as described by Eq. 12. The very small dispersion coefficients predicted under these conditions result from very high (calculated) degrees of polarization, and in general we find these difficult to obtain in practice.

Since our test systems are very small, fibers less than 1 mm in diameter and less than 1 m long, this small amount of dispersion is difficult to measure: that in the fiber is sometimes less

than that in the auxiliary apparatus, e.g. the UV monitor.

Early data were obtained simply by subtracting the variance of pulses in the auxiliary apparatus alone from that measured with the fiber in place:

$$\sigma_e^2 = \sigma_T^2 - \sigma_A^2 \tag{20}$$

with

$$\sigma_e^2 = 2\varepsilon_p \bar{t} r_p^2 / \bar{v}_m^2 \tag{21}$$

where

σ_T^2 = total variance under test conditions

σ_A^2 = variance for auxiliary apparatus without the fiber

σ_e^2 = experimental variance

$\bar{t}$ = mean protein residence time in fiber

The variance σ^2 is defined as the arithmetic mean of the square of the deviations from the mean. Equation 20 requires only linearity, stationarity, and negligible diffusional transport across system boundaries, in the auxiliary apparatus. These conditions should be met, but the use of Eq. 20 does not permit construction of the effluent curve corresponding to the fiber alone. We have now successfully developed a deconvolution technique based on a fast Fourier transform algorithm (Cooper (2); Higgins (3)), and this of course gives much more detailed information.

A representative result is shown in Fig. 12 for HSA. The ordinate, σ_e/σ_t, gives the deviation from theory as a function of observed retardation. Note that σ_t^2 is the predicted long-time variance from first-order theory. All show the same general behavior: smaller than calculated variances for r_p near unity but substantially larger than expected values at high retardation. We do not yet have a detailed explanation for these observations but are inclined to believe that:

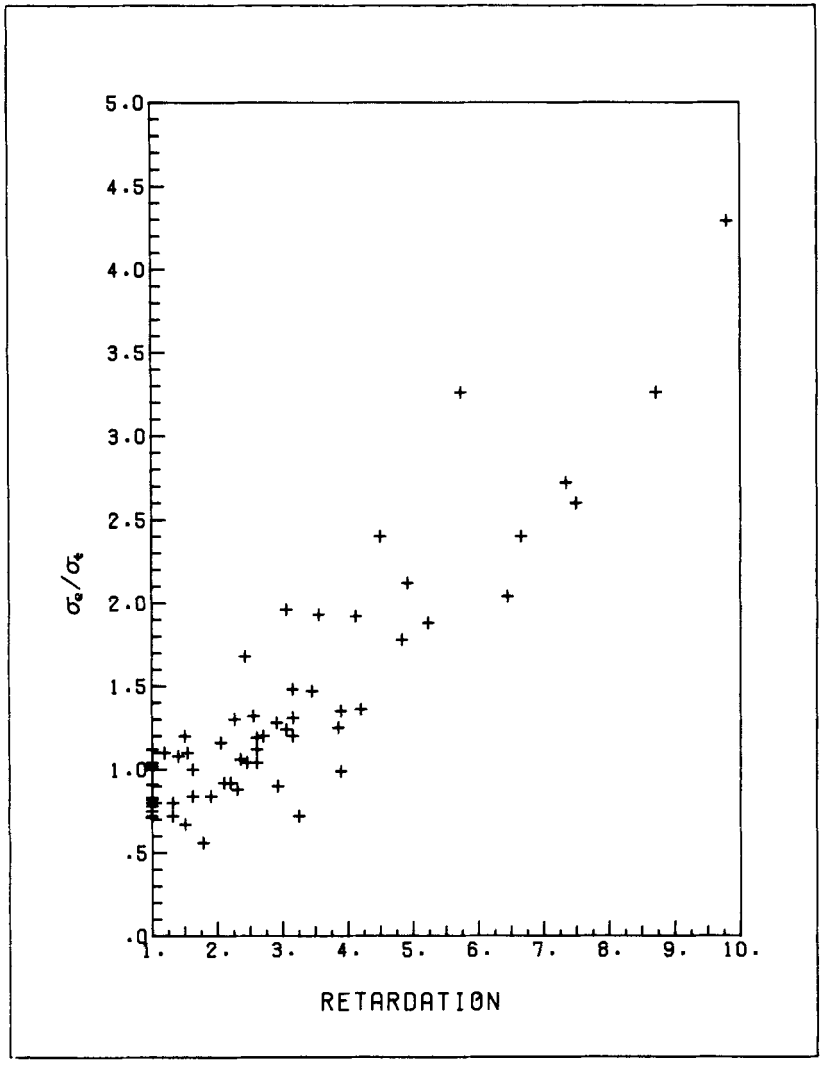

FIGURE 12. Axial dispersion of human serum albumin as a function of the retardation number, for a variety of experimental conditions. σ_e/σ_t is the ratio of the observed, deconvoluted standard deviation to the predicted standard deviation of the elution peak.

(1) Small variances at low r_p reflect transients since ε_p always progresses from $\mathcal{D}_{p_m}$ toward the much larger $(\varepsilon_p)_\infty$ with increasing time.

(2) Large variances at large r_p reflect small-ion polarization and other sources of non-ideal behavior we are presently investigating via the second-order modelling effort described below.

The investigation of dispersion is presently an active area of research. The effect of deconvolution is illustrated in Fig. 13 which compares raw effluent data with a deconvolution to eliminate dispersion in the auxiliary apparatus. It may be seen that the deconvoluted curve shows considerably less skewness.

Second-order Modelling

Here we attempt to improve on the first-order models, shown above to be inadequate for quantitative prediction of retardation, and we begin with a brief summary of those factors which must ultimately be taken into account. However, we are not yet in a position to consider all these factors in an effective way, and we, therefore, concentrate our attention on the diffusional processes occurring in the fiber lumen and confining wall. These are of primary importance, and we show in this discussion that even a much simplified one-dimensional diffusional model provides useful insight. A more extensive modelling effort, now in progress, will be discussed in a later paper.

Careful reading of the above discussions suggests that at least four kinds of behavior, ignored in the first-order model, can be expected to influence EPC in a significant way:

(1) Polarization of the small molecules and ions in the protein-buffer system and interaction between these and the proteins. Such polarization can occur both in the fiber lumen and wall, and polarization within the wall will be particularly important if the stationary membrane matrix has a fixed charge.

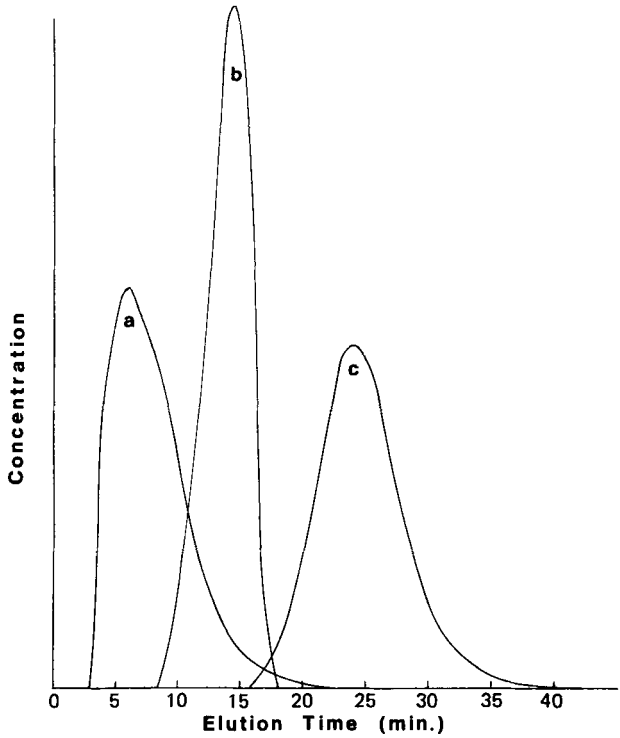

FIGURE 13. Deconvolution of an elution curve using the fast Fourier transform. Curve c is the observed elution curve for 50 µg of hemoglobin in 20 mM tris acetate pH 8.3 under an electric field of 17.3 v/cm. The flow rate is 21 µL/min. Curve a is the analogous output from the apparatus, with the fiber removed. Curve b is the deconvoluted result, representing the output from the fiber of an infintely sharp pulse of protein at the fiber inlet.

(2) Changes in effecive (electro-kinetic) charge and thermodynamic activity coefficients of the protein with position in the fiber lumen.

(3) Electro-osmotic water transport across the fiber wall.

(4) Specific chemical interactions between the protein and both the buffer and fiber surface.

All of these factors are deserving of attention, but we cannot presently deal effectively with all. We are at the greatest disadvantage with respect to the fourth where we do not yet have even the qualitative understanding needed to start an investigation. The others are relatively simple conceptually, and we are hampered primarily by lack of data: values of the diffusional parameters needed for numerical description. Lack of complete data for membrane hydraulic permeability is particularly serious since we have no means of estimating it at present; we must, therefore, defer investigation of water transport.

We are in a much better position with respect to diffusion coefficients, electrophoretic mobilities, and activity coefficients, and we, therefore, confine our present attention to the first two items in our list. Even here, however, we must make some geometric and physico-chemical simplifications.

Since we are primarily interested in retardation we consider continuous protein feed and calculate mean protein velocity relative to that of the solvent. Because prior modelling efforts (Shah et al. 12, Reis et al. 10) show very little sensitivity to geometry we adopt the one-dimensional model. Here the fiber lumen is treated as a rectangular channel of very large aspect ratio between membrane sheets. The external solution is assumed to be well stirred, so that polarization occurs only in the fiber lumen and the adjacent membranes.

In the lumen we consider the following six species to be present:

p^{ν_p}:	the protein, formally treated as an anion of charge ν_p
HX:	buffer
H^+(or OH^-):	hydrogen, or for alkaline solutions, hydroxide ions
X^-:	buffer anion
M^+:	buffer counter-ion
ω :	water

In the membrane phase we assume no protein to be present, but we now have the membrane matrix - which acts as a diffusing species and which can have a spatially immobilized electric charge. We are thus dealing in each phase with six diffusing species.

The diffusional behavior of such a system is in principle described by five independent flux equations, each of the form

$$\sum_{j\neq i}^{6} \frac{x_i x_j}{\mathcal{D}_{ij}} (v_j - v_i) = x_i \nabla_{T,p} \ln a_i + x_i \nu_i \frac{F}{RT} \nabla \phi \qquad (22)$$

where ν_i is the charge number of species i, a_i is the activity, F is the Faraday constant, R is the gas constant, and T is absolute temperature.

These contain 6(5)/2 = 15 independent diffusion coefficients, $\mathcal{D}_{ij}$, and 5 activity coefficients. This detail requires more information than is available. We simplify the description by neglecting diffusional interactions between solutes and neglecting activity-coefficient variations for the small solutes. We thus obtain five pseudo-binary Nernst-Planck equations, each of the form

$$N_i \doteq -c\mathcal{D}_{i\omega} \left[\frac{dx_i}{dz} + x_i \nu_i \frac{F}{RT} \frac{d\phi}{dz} \right] + \underline{x_i N_\omega} \qquad (23)$$

$$(i = HX, H^+, X^-, M^+, \neq \omega, p)$$

$$N_p \doteq -c\mathcal{D}_{p\omega} \left[\left(1 + \frac{\partial \ell n \gamma_p}{\partial \ell n x_p} \right) \frac{dx_p}{dz} + x_p m \nu_p \frac{F}{RT} \frac{d\phi}{dt} \right] \qquad (24)$$

where c is the total molar concentration, and m is a correction to the net electric charge of the protein which includes the electrophoretic effect as approximated by Henry's equation (15). The underlined term in equation 23 is ignored at our present level of understanding. The flux equation for the membrane is not used since the restraining force acting on the membrane is not considered. We further assume the activity coefficient of the protein, γ_p, can be calculated from Donnan equilibrium theory (15):

$$\left(1 + \frac{\partial \ell n \gamma_p}{\partial \ell n x_p} \right) = \frac{1}{RT} \left(1 - \phi_p \right) \frac{\partial \pi}{\partial c_p} \qquad (25)$$

where Φ_p is the protein volume fraction, and

$$\frac{\partial \pi}{\partial c_p} \doteq RT\left(1 + \frac{\nu_p{}^2 x_p}{2(x_x + \nu_p x_{p/2})}\right) \tag{26}$$

Several restraints are still needed to specify the problem. Here we include,

$$N_\omega = 0 \tag{27}$$

$$\sum_i^n x_i = 1 \tag{28}$$

$$\sum_i^n \nu_i x_i = 0 \tag{29}$$

$$x_H x_X / x_{HX} = K_{eq}/c \tag{30}$$

$$\sum_i^n N_i \nu_i F = I \tag{31}$$

where K_{eq} is the buffer equilibrium constant, and I is the current density. At the interfaces we assume the activities of small ions are constant:

$$x_X x_H\Big|_I = x_X x_H\Big|_{II} \tag{32}$$

$$x_X x_M\Big|_I = x_X x_M\Big|_{II} \tag{33}$$

In addition, ν_p may be expressed as a function of x_H from titration data when it is available.

The boundary conditions for the model specifies the concentrations of the small solutes at both outer interfaces for the three phase system. It is convenient to also specify ϕ and x_p at one boundary. However, the differential equations are only first order, and this over-specification of the boundary conditions requires us to keep two variables unknown, and we have chosen two of the small ion fluxes. A shooting-type iterative method is required to solve these differential equations simultaneously, where the two unknown fluxes are corrected until all boundary conditions are met.

Our initial calculations were made with the somewhat simpler model of the four component system: protein, water, cation, and anion. This model contains only one unknown flux which must be corrected to match the boundary conditions. The charge of the protein can also be assumed to remain constant since hydrogen ion is not considered to be a component. The results presented in this paper are primarily from this model.

Calculations with the binary electrolyte system, were designed to approximate ovalbumin of pH 5.5 in electrolytes of concentrations, .004 to .010 M. The cation and anion were assumed to have equivalent transport properties

$$\mathcal{D}_{X\omega} = \mathcal{D}_{M\omega} = 1.0 \times 10^{-5} \text{cm}^2/\text{sec}.$$

$$\mathcal{D}_{XR} = \mathcal{D}_{MR} = 3.33 \times 10^{-6} \text{cm}^2/\text{sec}.$$

where $\mathcal{D}_{iR}$ refer to the effective diffusivities in the membrane phases. The charge number of ovalbumin was assumed to be -10. A Runge-Kutta fourth-order integration method was found suitable for integration of the equations, provided the integration proceeded from low to high protein concentrations.

Figure 14 compares the retardation results of this model with the predictions of the earlier model of Reis et al. (10). Typical loads of ovalbumin are used: for curves A-C, 0.05% on a mass basis, and 0.1% for curves D-F. Curves A and D result from the simple case of an uncharged membrane and no activity correction for the protein. Curves B and E include a slight negative charge on the membrane of 0.001 M, and curves C and F also include protein activity corrections.

It is apparent that the nature of the membrane, the mass load of protein, and the activity coefficient of the protein are all important parameters affecting retardation. However, the most important effect appears to be the polarization of the small ions in the protein boundary layer, which significantly reduces the electric field in this region. It is this effect alone, which accounts for curves A and D.

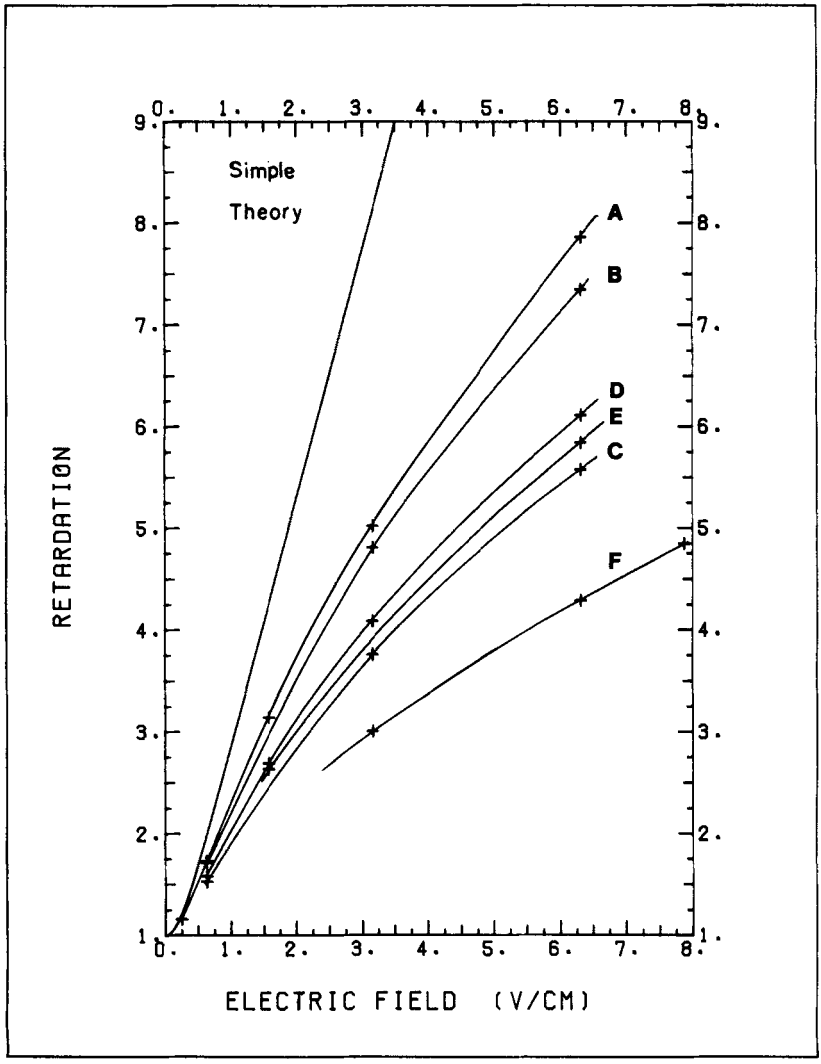

FIGURE 14. Comparison of second-order binary electrolyte model with theory of Reis, et al. (10). Parameters were adjusted to correspond to ovalbumin at pH 5.5 in a 4 mM. buffer, as in Figure 6. See text for an explanation of different curves.

Figure 15 demonstrates that the electrolyte concentration determines to a large extent how large the deviations from the first-order theory may be. This figure is analogous to Figure 14, but the electrolyte concentration is larger, 0.100 M. Curve A is for ovalbumin at 0.05% concentration with an uncharged membrane, and curve B includes a protein activity correction.

In Figure 16 a comparison is made between curve A of Figure 14 and an analogous curve resulting from the six component buffer system model. The close correspondence is noteworthy, although several effects including the pH dependence of the protein charge have not been included.

The protein boundary layer that is predicted by this new modeling effort is shown in Figure 17, in comparison with the exponential prediction of Reis et al. (10). Similar results have been observed for all the cases studied and indicate the protein boundary layer is thicker and less concentrated than earlier predicted. This would qualitatively give larger dispersions, which have yet to be calculated.

The initial results of this modelling effort are encouraging in that theoretical predictions are now in qualitative agreement with most of the available data, shown for the case studied in Figure 6. Hopefully, more quantitative predictions of EPC behavior will be forthcoming, as transport models incorporating specific properties of the buffer, protein, and membrane phases are introduced.

CONCLUSIONS

The experimental results presented give an unbiased comparison with theory, and show that the first-order models currently used are inadequate. Improvements of the EPC apparatus and the addition of a micro-processor have allowed more precise control and measurement of the process. Measurements of fiber wall conductivities have allowed the determination of the intraluminal electric field.

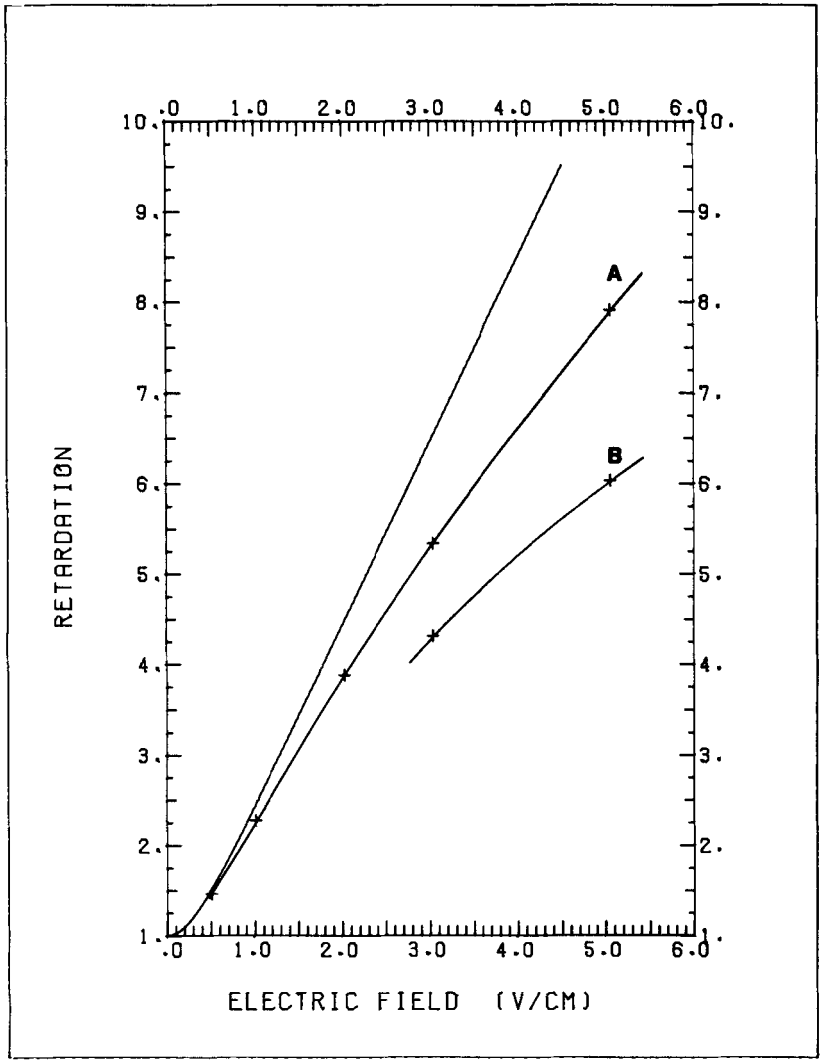

FIGURE 15. Comparison of second-order binary electrolyte model with theory of Reis, et al. (10) in 10mM electrolyte. Parameters are the same as in Figure 14, except for the electrolyte concentration. See text for an explanation of the labeled curves.

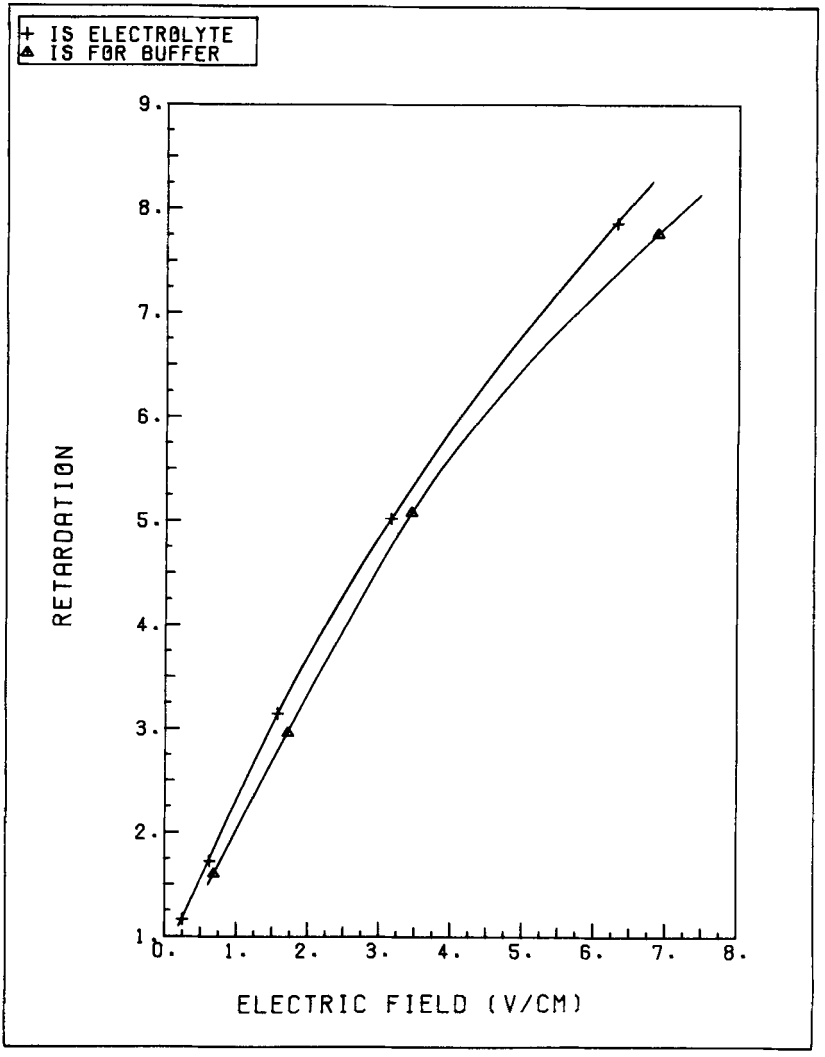

FIGURE 16. Comparison of binary electrolyte model with the 6 component buffer model. The electrolyte model curve is A from Figure 14 with ν_p = -10. The buffer model curve is given for 4mM sodium acetate at pH 5.5 with a fixed charge on ovalbumin = -7.87.

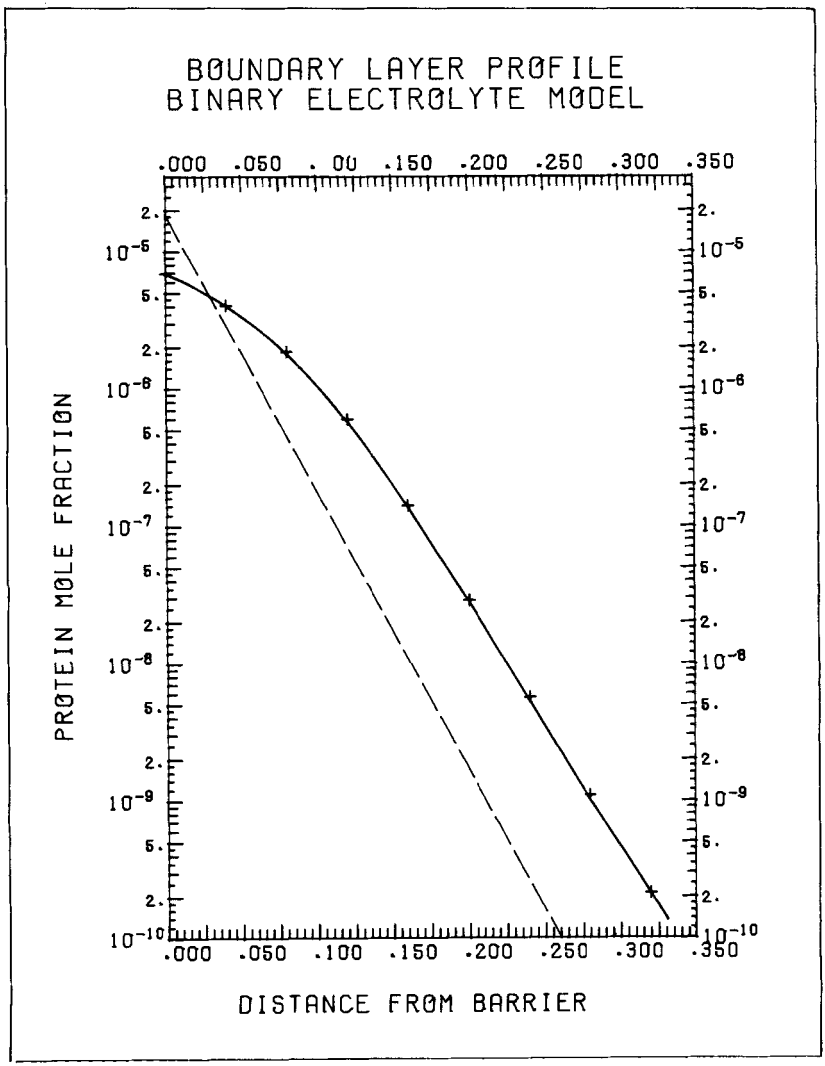

FIGURE 17. Ovalbumin boundary layer profile given from the binary electrolyte model for .05% ovalbumin in 4 mM electrolyte with E = 6.3 v/cm. The dashed line is the exponential prediction of Reis et al. (10) for the same retardation number equal to 7.861.

It has been found that the buffer ions and their concentrations, the mass load of protein, and fiber wall composition have profound influences on the retardation which deviates from the first-order model; the observed dispersions of deconvoluted elution peaks are larger than predicted, deviating more at higher retardation.

A second-order modelling effort has begun which includes the interactions of multicomponent transport. Initial results indicate this model may be able to account for the major factors affecting performance.

ACKNOWLEDGEMENTS

We are indebted to the work and valuable experience furnished by Edward H. Kmiotek, in dealing with materials as complex as proteins, and to technicians, LeAnn Birklid and Wendy Aldrich. We are also indebted to the National Institute of Health for funds furnished under grant #GM-24747.

REFERENCES

1. A.S. Chiang, E.H. Kmiotek, S.M. Langan, P.T. Noble, J.F.G. Reis, and E.N. Lightfoot, Sep. Sci. & Tech. 14, 453 (1979).

2. J.W. Cooper, The Minicomputer in the Lab.,Wiley-Interscience, New York (1977).

3. R.J. Higgins, Am. J. of Phys. 44, 766 (1976).

4. J.G. Kirkwood, R.A. Brown, J.A.C.S. 74, 1056 (1952).

5. H.L. Lee, E.N. Lightfoot, Sep. Sci. 11, 417 (1976).

6. E.N. Lightfoot, Transport Phenomena and Living System, Wiley-Interscience, New York (1974).

7. E.N. Lightfoot, A.S. Chiang, P.T. Noble, Ann. Rev. Fluid Mech. 13 351, (1981).

8. D. Ramkrishna, N.R. Amundson, Chem. Eng. Sci. 29, 1353 (1974).

9. J.F.G. Reis, E.N. Lightfoot, A.I.Ch.E.J. 22, 779 (1976).

10. J.F.G. Reis, D. Ramkrishna, E.N. Lightfoot, A.I.Ch.E.J. 24, 679 (1978).

11. A.G. Schnek, W.A. Schroeder, J.A.C.S. 83, 1472 (1961).

12. A.B. Shah, J.F.G. Reis, E.N. Lightfoot, Sep. Sci. & Tech. 14, 475 (1979).

13. A.F. Taggert, Handbook of Mineral Dressing, Wiley, New York (1953).

14. T. Takahashi, W.N. Gill, Chem. Eng. Commun. 5, 367 (1980).

15. C. Tanford, Physical Chemistry of Macromolecules, Wiley, New York (1961).